ChemPubSoc Europe

DOI: 10.1002/chem.201304437

CHEMISTRY A European Journal Full Paper

Supramolecular Chemistry

Solvent-Dependent Self-Assembly Behaviour and Speciation Control of Pd_6L_8 Metallo-supramolecular Cages

James J. Henkelis, Julie Fisher, Stuart L. Warriner, and Michaele J. Hardie*[a]

Abstract: The C_3-symmetric chiral propylated host-type ligands (±)-*tris*(isonicotinoyl)-*tris*(propyl)-cyclotricatechylene (**L1**) and (±)-*tris*(4-pyridyl-4-benzoxy)-*tris*(propyl)-cyclotricatechylene (**L2**) self-assemble with Pd^{II} into $[Pd_6L_8]^{12+}$ metallo-cages that resemble a stella octangula. The self-assembly of the $[Pd_6(\mathbf{L1})_8]^{12+}$ cage is solvent-dependent; broad NMR resonances and a disordered crystal structure indicate no chiral self-sorting of the ligand enantiomers in DMSO solution, but sharp NMR resonances occur in MeCN or $MeNO_2$. The $[Pd_6(\mathbf{L1})_8]^{12+}$ cage is observed to be less favourable in the presence of additional ligand, than is its counterpart, where L = (±)-*tris*(isonicotinoyl)cyclotriguaiacylene (**L1 a**). The stoichiometry of reactant mixtures and chemical triggers can be used to control formation of mixtures of homoleptic or heteroleptic $[Pd_6L_8]^{12+}$ metallo-cages where L = **L1** and **L1 a**.

Introduction

The self-assembly of metallo-supramolecular assemblies from multifunctional ligands and transition metal cations is well established and has yielded a variety of cage-like species.[1] These may have hollow interiors where additional guest molecules or ions may be bound, and their ability to act as host assemblies means that a number of metallo-cage systems are being developed as nano-scale hosts and reaction vessels, with applications including the trapping of reactive species,[2] enabling unusual reactivities and catalysis[3] and templating nanoparticle formation.[4] Metallo-cages, also known as coordination cages, are examples of host assemblies where the individual molecular or ionic components do not necessarily have host-function themselves, which is a distinction from molecular hosts, which are individual molecules capable of binding guests. A theme of our research is the self-assembly of metallo-cages that utilise ligand-functionalised molecular hosts, in particular those based on cyclotriveratrylene (CTV). Other types of molecular hosts have also been employed to this effect, most particularly from the calixarene family.[5]

Cyclotriveratrylene is a relatively rigid and pyramidal-shaped host with an open upper rim.[6] Both CTV and its chiral analogue cyclotriguaiacylene (CTG) can be converted into extended-armed host molecules through upper rim functionalisation. Metallo-supramolecular assemblies of ligand functionalised CTV-analogues include single-cage and double-cage catenating $[M_3L_2]$ capsule-like metallo-cryptophanes,[7] $[M_4L_4]$ and $[M_6L_4]$ tetrahedra,[8] $[M_6L_8]$ stella octangula assemblies,[9] and a self-entangled $[M_4L_4]$ cube.[10] The largest metallo-cages involving CTV-type ligands are the $[Pd_6L_8]^{12+}$ stella octangula assemblies that occur with ligands that have 4-pyridyl groups appended, such as **L1 a**, **L1 b** and **L2 a** (Scheme 1).[9] The crystal structure of the previously reported $[Pd_6(\mathbf{L1\,a})_8]^{12+}$ stella octangula[9b] has six Pd^{II} cations arranged in an octahedron with the eight **L1 a** ligands taking up the octahedron's faces giving a 3 nm sized cage assembly (Scheme 1). The pyramidal aspect of the ligands gives the cage a spiked appearance (Scheme 1) similar to a stella octangula, which is the first stellation of an octahedron. Although crystals of $[Pd_6(\mathbf{L1\,a})_8]\cdot 12\,NO_3$ are racemic, each stella octangula cage is homochiral, being composed of only one of the two **L1 a** enantiomers.[9b] An analogous, octomeric CTV-based cube, assembled through labile covalent bonds, has been reported by Warmuth.[11]

The previously reported $[Pd_6L_8]^{12+}$ stella octangula cages are only soluble in dimethylsulfoxide (DMSO), which limits their potential as nano-scale hosts. In a bid to improve the solubility of these cages, we targeted the propylated ligands, *tris*(isonicotinoyl)-*tris*(propyl)-cyclotricatechylene (**L1**), and *tris*(4-pyridyl-4-benzoxy)-*tris*(propyl)-cyclotricatechylene (**L2**), shown in Scheme 1. The vast majority of known CTV analogues with mixed upper rim substituents feature either a methoxy or hydroxyl group as one of the substituents,[6] examples of other combinations of mixed upper rim groups are much rarer.[12,13]

Results and Discussion

Propylated-cyclotriguaiacylene **2** (*p*-CTG) was prepared from propylated-cyclotriveratrylene **1** (*p*-CTV),[14] which was demethylated using lithium diphenylphosphide generated in situ by lithiation of diphenylphosphine with *n*-butyl lithium (Scheme 2).[13] Lithium diphenylphosphide selectively demethylates aryl methyl ethers over other alkyls, and Collet had previously used the same approach for hetero-functionalisation of

[a] J. J. Henkelis, Dr. J. Fisher, Dr. S. L. Warriner, Prof. M. J. Hardie
School of Chemistry, University of Leeds
Woodhouse Lane, Leeds, LS2 9JT (UK)
E-mail: m.j.hardie@leeds.ac.uk

Supporting information for this article is available on the WWW under http://dx.doi.org/10.1002/chem.201304437.

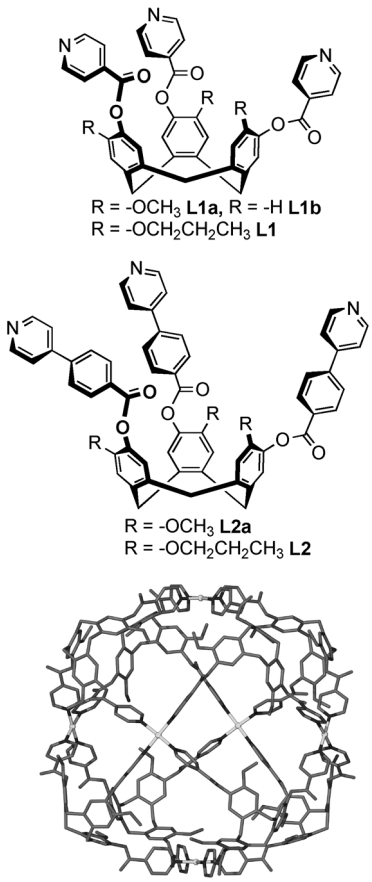

Scheme 1. Previously reported and target (**L1**, **L2**) pyramidal tripodal ligands with 4-pyridyl donor groups and the crystal structure of $[Pd_6(\mathbf{L1a})_8]^{12+}$ from ref. [9b].

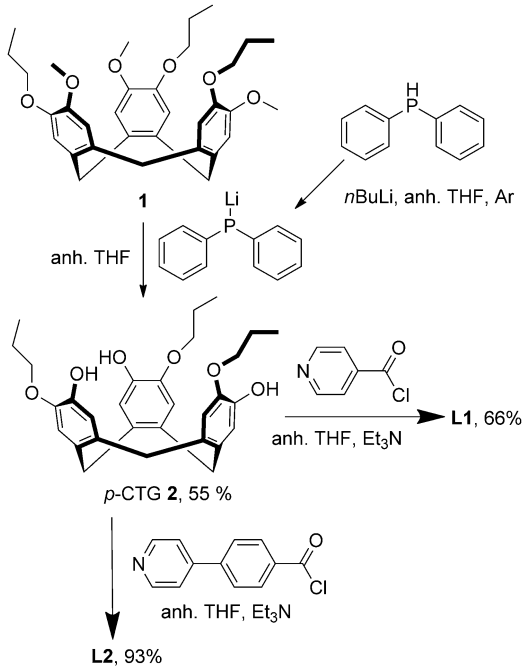

Scheme 2. Synthesis of the propylated CTG ligands **L1** and **L2**.

the CTV framework.[13] The ^{1}H NMR spectrum of *p*-CTG displayed the characteristic diastereotopic resonances of the *endo*- and *exo*-protons of the tribenzo[*a,d,g*]cyclononatriene core at 3.31 and 4.56 ppm ([D_6]DMSO), respectively. *p*-CTG was highly soluble in common organic solvents and was observed to act as a gelator for the solvents dichloromethane, chloroform, nitromethane, acetonitrile and tetrahydrofuran. Gelator behaviour of CTV analogues and derivatives has been previously observed.[15] *p*-CTG was converted to **L1** and **L2** using adapted versions of previously reported syntheses,[9a,16] with each ligand being obtained as a racemic mixture in high yields according to Scheme 2.

The crystal structure of **L1** was determined from its clathrate complex **L1**·0.5 ($MeNO_2$)·1.5 (H_2O). The asymmetric unit features one molecule of **L1**, a $MeNO_2$ disordered across an inversion centre, and three poorly resolved regions of solvent, modelled as partial water molecules. **L1** deviates from strict molecular C_3-symmetry and all ester groups are oriented with the carbonyl groups away from the cavity of the cyclononatriene core (Figure 1). The closest aromatic separation between the ligands

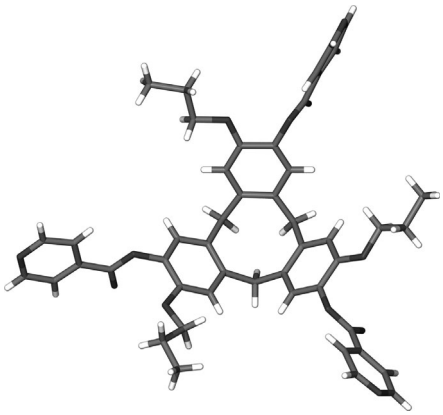

Figure 1. From the crystal structure of complex **L1**·0.5 ($MeNO_2$)·1.5 (H_2O).

is 4.4 Å, which is too long to suggest any π–π interactions. There are, however, π–H intermolecular interactions between the terminal methyl and pyridyl groups of nearby ligands, with C–H···pyridine separations of 3.06 Å. The overall crystal lattice has a bilayer-like arrangement of sheets of **L1** ligands separated by solvent (Figure S4 in the Supporting Information).

Self-assembly of $[M_6L_8]^{12+}$ stella octangula cages

Self-assembly of the propylated stella octangula, $[Pd_6(\mathbf{L1})_8]^{12+}$, was achieved through combination of eight equivalents of racemic ligand **L1** with six equivalents of PdX_2 (where X = NO_3^-, BF_4^- or $CF_3CO_2^-$) in a variety of different solvents, namely DMSO, DMF, MeCN, $MeNO_2$ and, surprisingly, a 9:1 mixture of water/MeCN (the last observed only by mass spectrometry). Electrospray mass spectrometry (ESI-MS) studies of solution mixtures of $[Pd(MeCN)_4](BF_4)_2$ and **L1** shows rapid formation of the stella octangula cage with mass peaks of (*m/z*) 1949.6343, 1542.0858, 1270.3947 and 1076.7391 being attribut-

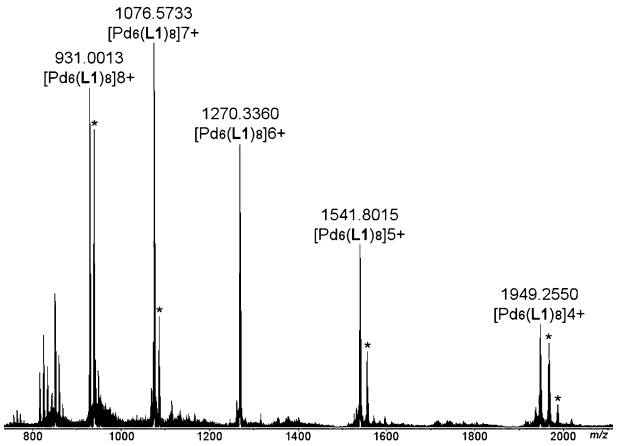

Figure 2. ESI-MS from mixture of **L1** and $[Pd(MeCN)_4](BF_4)_2$, showing various $\{[Pd_6(\mathbf{L1})_8]\cdot m(BF_4)\}^{12-m+}$ ions, asterisk indicates a cage-DMSO adduct.

ed to $\{[Pd_6(\mathbf{L1})_8]\cdot 8\,BF_4\}^{4+}$, $\{[Pd_6(\mathbf{L1})_8]\cdot 7\,BF_4\}^{5+}$, $\{[Pd_6(\mathbf{L1})_8]\cdot 6\,BF_4\}^{6+}$ and $\{[Pd_6(\mathbf{L1})_8]\cdot 5\,BF_4\}^{7+}$, respectively (Figure 2). Cage-DMSO adducts were also observed, for instance in the 4+ charge state, mass peaks of 1948.9994, 1968.5019 and 1988.5064 were attributed to $\{[Pd_6(\mathbf{L1})_8]\cdot 8\,BF_4\}^{4+}$, $\{(DMSO)\subset[Pd_6(\mathbf{L1})_8]\cdot 8\,BF_4\}^{4+}$ and $\{(DMSO)_2\subset[Pd_6(\mathbf{L1})_8]\cdot 8\,BF_4\}^{4+}$, respectively. Similar mass spectra were seen in all solvents utilised and were independent of the counter anion used, and the spectra did not substantially change when monitored over a period of weeks (Figures S8 and S11 in the Supporting Information).

2D diffusion-ordered spectroscopic experiments (DOSY) in DMSO indicated a single large species in solution with a diffusion coefficient of $0.439\times10^{-10}\,m^2\,s^{-1}$ (Figure S11 in the Supporting Information). Based on the diffusion coefficient of free ligand, $1.293\times10^{-10}\,m^2\,s^{-1}$, a $D_{complex}/D_{ligand}$ ratio of 0.33:1 was established which, through the Stokes–Einstein relationship, was estimated to give a hydrodynamic radius (*r*) of 23.4 Å. This is larger than the hydrodynamic radius of 19.4 Å that was measured for $[Pd_6(\mathbf{L1a})_8]^{12+}$,[9b] consistent with the longer and more conformationally flexible propyl chains.

The 1D ^{1}H NMR spectra of the $[Pd_6(\mathbf{L1})_8]^{12+}$ cage indicated that aspects of the solution-phase self-assembly are solvent-dependent. All ^{1}H NMR spectra show strong coordination-induced downfield shifting of the pyridyl *ortho* and *meta* protons, and upfield shifts of propyl group protons. Those obtained in $[D_6]$DMSO, or $[D_7]$DMF, display broad peaks that do not sharpen over several weeks of monitoring (Figure 3a and Figure S9 in the Supporting Information). Heating the $[D_6]$DMSO solution to 60 °C for 18 h before monitoring does not lead to any changes in the spectrum. Heating the Pd^{II} precursor in $[D_6]$DMSO for 1 h prior to cooling to room temperature then addition of the ligand also results in no variation. The spectrum obtained in $[D_3]$MeCN, however, initially shows broad resonances but this resolves to a sharper spectrum over a period of three days (Figure 3b and Figure S12 in the Supporting Information). The spectra do not sharpen up entirely and the DOSY NMR in $[D_3]$MeCN indicates the presence of a second species in solution of very similar size (Figure S13 in the Supporting Information). A sharp ^{1}H NMR spectrum is immediately obtained in $[D_3]MeNO_2$, however, the cage formation was not quantitative as there is also free ligand in solution (Figure S14 in the Supporting Information). For all solvents, ESI-MS studies are dominated by the $[Pd_6(\mathbf{L1})_8]^{12+}$ species and do not vary when monitored over days or weeks.

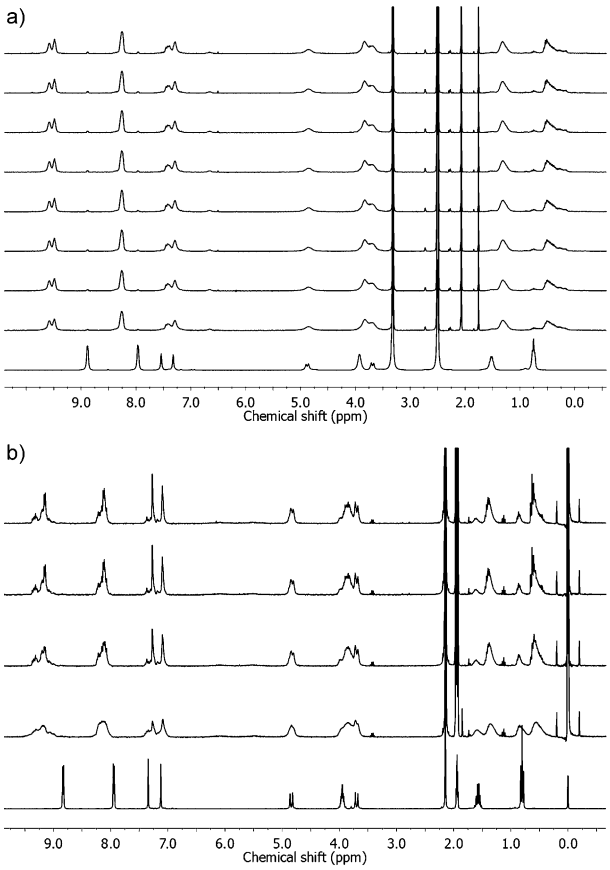

Figure 3. ^{1}H NMR spectra of ligand **L1** (bottom trace) and the corresponding stella octangula complex $[Pd_6(\mathbf{L1})_8]\cdot 12\,BF_4$ monitored over a week of standing the solution: a) $[D_6]$DMSO solution; b) $[D_3]$MeCN (time increases on vertical scale).

We propose that the broadened spectra are indicative of a mixture of $[Pd_6(\mathbf{L1})_8]^{12+}$ cages, which are not chirally resolved, while sharpened spectra indicate chiral self-sorting. Hence, $[Pd_6(\mathbf{L1})_8]^{12+}$ self-sorts rapidly in $MeNO_2$, more slowly and incompletely in MeCN, but not over a timescale of many weeks in DMSO or DMF. In the original $[Pd_6(\mathbf{L1a})_8]^{12+}$ stella octangula,[9] sharp ^{1}H NMR spectra are obtained in $[D_6]$DMSO and the crystal structure of the nitrate salt showed chiral self-sorting as each $[Pd_6(\mathbf{L1a})_8]^{12+}$ cage was crystallographically ordered and contained only one ligand enantiomer (Scheme 1).[9b]

Single crystals of the BF_4^- salt of $[Pd_6(\mathbf{L1})_8]^{12+}$ were obtained from DMSO solution, and X-ray diffraction data were collected using synchrotron radiation. The structures of $[Pd_6(\mathbf{L1a})_8]^{12+}$ and $[Pd_6(\mathbf{L1})_8]^{12+}$ are not isomorphic, however, both crystallise with tetragonal unit cells.[17] The structure of $[Pd_6(\mathbf{L1})_8]\cdot 12\,(BF_4)$ gives Pd^{II} positions in a near octahedral arrangement with Pd···Pd separations 16.3 Å, comparable with the symmetry and Pd···Pd separation (16.6 Å) observed for $[Pd_6(\mathbf{L1a})_8]^{12+}$. The

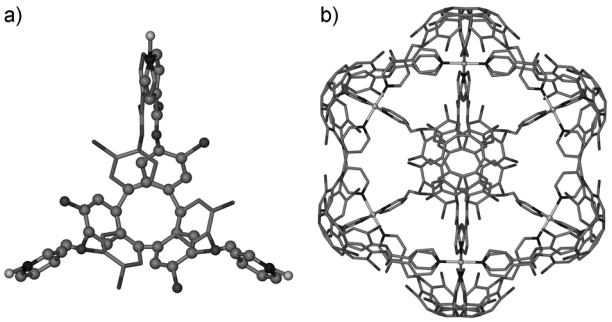

Figure 4. From the crystal structure of $[Pd_6(\mathbf{L1})_8]\cdot 12(BF_4)\cdot 2(H_2O)$. a) Detail showing disordered ligand bridging between three Pd^{II} centres with the superposition of both ligand enantiomers, one enantiomer is shown in ball-and-stick to highlight; b) the disordered $[Pd_6(\mathbf{L1})_8]^{12+}$ stella octangula cage.

bridging **L1** ligand, however, is completely disordered within the structure. The disorder has been modelled such that each full ligand position is a superposition of both ligand enantiomers (Figure 4 and Figure S6 in the Supporting Information). This is consistent with $[Pd_6(\mathbf{L1})_8]^{12+}$ cages forming from a mixture of ligand enantiomers, with the apparent superposition an average ligand position across all unit cells. The ^{1}H NMR spectrum of isolated single crystals that were redissolved in $[D_6]$DMSO is identical to the original spectrum shown in Figure 3a, supporting the notion that the broadened spectra reflect a mixture of cage stereoisomers.

Another interpretation is that broadened spectra are indicative of incomplete self-assembly to the symmetrical $[Pd_6(\mathbf{L1})_8]^{12+}$ cages, and that we are observing lower symmetry variants with the same stoichiometry. Yoneya and co-workers have recently reported molecular dynamics simulations of the self-assembly of $[Pd_6L_8]$ spherical cages where L is the achiral tripodal ligand 1,3,5-*tris*(methyl-4-pyridyl)-benzene.[18] In that study, lower symmetry complexes were found leading up to the formation of the symmetrical $[Pd_6L_8]$. Given the short lifetimes of these species, and the high symmetry—albeit disordered—cage found in the crystal structure, we find this to be a less plausible explanation for this system.

Homochiral self-sorting in metallo-supramolecular assemblies, where ligand enantiomers recognise one another from a racemic mixture, has been previously reported both for stella octangula cages[9] and for other systems,[19] and includes examples in which sorting from a stereomeric mixture occurs over several days.[19c] However, systems in which such self-sorting is dependent on what solvent is used are a much rarer occurrence, and we are unaware of another example that parallels this one. Solvent-effects have been reported for equilibria between diastereomers of the atrane structure of a hemicryptophane–oxidovanadium complex,[20] and solvent may affect stereoselectivity in organic synthesis.[21]

A platinum(II) congener, $[Pt_6(\mathbf{L1})_8]\cdot 12\,ClO_4$, is formed but not in quantitative yields. The ^{1}H NMR spectrum in $[D_6]$DMSO was symmetrical and displayed the characteristic downfield shifts of the pyridyl resonances, similar to the palladium(II) analogue described above; yet, due to the decreased lability of the metal centre, conversion to the cage was measured to be only 75%, despite heating to 70 °C, overnight, then standing for a week (Figure S15 in the Supporting Information). Mass peaks of (*m/z*) 1371.6856, 1665.9895 and 2107.4224 were observed and corresponded to $\{[Pt_6(\mathbf{L1})_8]\cdot 6\,ClO_4\}^{6+}$, $\{[Pt_6(\mathbf{L1})_8]\cdot 7\,ClO_4\}^{5+}$ and $\{[Pt_6(\mathbf{L1})_8]\cdot 8\,ClO_4\}^{4+}$, respectively.

The treatment of eight equivalents of **L2** with six equivalents of $[Pd(MeCN)_4](BF_4)_2$ in DMSO likewise results in the rapid and quantitative formation of the Pd_6L_8 stella octangula (Figures S16–S18 in the Supporting Information). The 1D NMR spectrum of the cage in $[D_6]$DMSO is broad, with the pyridyl *ortho*-resonances shifted strongly downfield due to the pyridyl-palladium coordination, again consistent with cage formation but not self-sorting. DOSY NMR spectroscopy showed the diffusion of one large species in solution with a diffusion coctjl;efficient of $0.348\times10^{-10}\,m^2s^{-1}$, and ESI-MS gives mass peaks of (*m/z*) 910.0709 and 1020.8581 corresponding to $\{[Pd_6(\mathbf{L2})_8]\cdot 2\,BF_4\}^{10+}$ and $\{[Pd_6(\mathbf{L2})_8]\cdot 3\,BF_4\}^{9+}$, respectively.

Guest binding and chemical disassembly–reassembly

Preliminary host–guest binding studies of $[Pd_6(\mathbf{L1})_8]^{12+}$ monitored by ESI-MS indicates that guest *o*-carborane association occurs in DMF solution. Each $[Pd_6(\mathbf{L1})_8]\cdot n(BF_4)^{12-n}$ charge state showed multiple guest adducts. For instance, two *o*-carborane adducts were observed as part of the 5+ mass-charge envelope, with mass peaks of (*m/z*) 1541.8719, 1570.4850 and 1598.4942 corresponding to $\{[Pd_6(\mathbf{L1})_8]\cdot 7\,BF_4\}^{5+}$, $\{(\text{carborane})\subset[Pd_6(\mathbf{L1})_8]\cdot 7\,BF_4\}^{5+}$ and $\{(o\text{-carborane})_2\subset[Pd_6(\mathbf{L1})_8]\cdot 7\,BF_4\}^{5+}$, respectively. Similar host–guest phenomena were displayed for the 8, 7 and 6+ charge states. Crystal structures of solid-state *o*-carborane and halogenated carborane anion host–guest complexes with CTVs have been previously shown, and usually feature C–H···π hydrogen bonding from the acidic carborane C–H group.[22]

The $[Pd_6(\mathbf{L1})_8]^{12+}$ stella octangula cage can be chemically disassembled and reassembled. According to NMR spectroscopy observations (Figure S20 in the Supporting Information), treatment of the preformed cage with 24 equivalents of 4,4′-dimethylaminopyridine (DMAP) resulted in the quantitative disassembly of the cage and generated free **L1**, alongside $[Pd(DMAP)_4]\cdot 2\,BF_4$. This occurs as DMAP is a stronger Lewis base than the pyridyl group due to the inductive effects of the amine group. The cage was quantitatively reassembled by subsequent addition of 24 equivalents of *para*-toluenesulfonic acid (TsOH) to regenerate the $[Pd_6(\mathbf{L1})_8]\cdot 12\,BF_4$ assembly and H^+-DMAP (Figure S20 in the Supporting Information). This demonstrates scope for application in cargo delivery and the selective sequestration or release of guests upon initiation by a localised trigger. The DMAP-TsOH chemical trigger has been previously used with metallo-cages and in other supramolecular systems, such as switchable molecular shuttles.[23]

Ligand exchange and speciation control

The availability of the sterically and interactionally similar ligand pairs, **L1a**/**L1** and **L2b**/**L2**, all of which form a $[Pd_6L_8]^{12+}$ cage, allows us to study the formation of $[Pd_6L_8]^{12+}$ cages from

a mixture of ligands, as well as any ligand exchange that occurs between the cages.

Heteroleptic $[Pd_6(\mathbf{L1})_{8-n}(\mathbf{L1\,a})_n]^{12+}$ and $[Pd_6(\mathbf{L2})_{8-n}(\mathbf{L2\,a})_n]^{12+}$ cages can be formed. The combination of six equivalents of $[Pd(MeCN)_4](BF_4)_2$ with four equivalents of each of **L1** and **L1 a** was allowed to stand, overnight. Electrospray mass spectrometry indicated heteroleptic $[Pd_6(\mathbf{L1})_{8-x}(\mathbf{L1\,a})_x]\cdot 12\,BF_4$ cage formation, where each mass-charge envelope for a given charge state was identified to be a near statistical mixture of ligand combinations. For example, the mass spectra for the 5+ mass-charge envelope displayed mass peaks of (*m/z*) 1424.7916, 1440.9024, 1457.9135, 1474.3383, 1491.3380 and 1510.6050, which corresponded to $\{[Pd_6(\mathbf{L1})_1(\mathbf{L1\,a})_7]\cdot 7\,BF_4\}^{5+}$, $\{[Pd_6(\mathbf{L1})_2(\mathbf{L1\,a})_6]\cdot 7\,BF_4\}^{5+}$, $\{[Pd_6(\mathbf{L1})_3(\mathbf{L1\,a})_5]\cdot 7\,BF_4\}^{5+}$, $\{[Pd_6(\mathbf{L1})_4(\mathbf{L1\,a})_4]\cdot 7\,BF_4\}^{5+}$, $\{[Pd_6(\mathbf{L1})_5(\mathbf{L1\,a})_3]\cdot 7\,BF_4\}^{5+}$ and $([Pd_6(\mathbf{L1})_6(\mathbf{L1\,a})_2]\cdot 7\,BF_4\}^{5+}$, respectively. Once formed, there was no evidence of subsequent ligand exchange over several weeks of monitoring, and the mass spectra procured were consistent across DMSO, DMF and MeCN. The ^{1}H NMR spectrum in [D_6]DMSO was broad and was not observed to sharpen. The formation of a mixture of heteroleptic cages was also observed from similar experiments with the **L2 a**/**L2** ligand pair, and the ESI-MS obtained is shown in Figure 5.

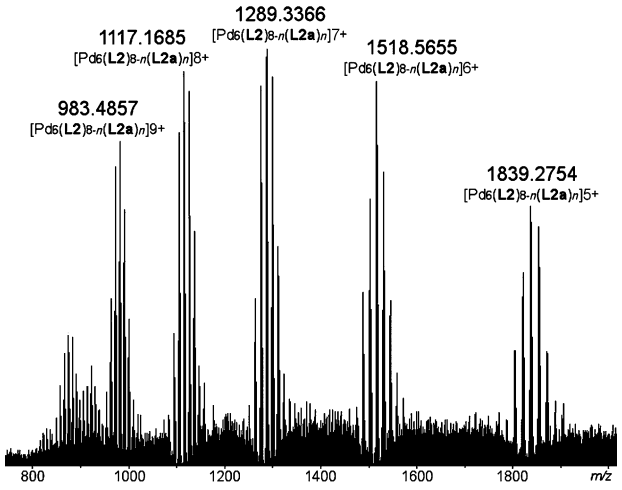

Figure 5. ESI-MS showing formation of heteroleptic $[Pd_6(\mathbf{L2})_{8-n}(\mathbf{L2\,a})_n]$ cages from a 4:4:6 mixture of **L2**/**L2 a**/$[Pd(MeCN)_4](BF_4)_2$. Different charge states show different $\{[Pd_6(\mathbf{L2})_{8-n}(\mathbf{L2\,a})_n]\cdot m(BF_4)\}^{12-m+}$ series.

A 1:1 mixture of preformed $[Pd_6(\mathbf{L1})_8]\cdot 12\,(BF_4)$ and $[Pd_6(\mathbf{L1\,a})_8]\cdot 12\,(BF_4)$ in [D_6]DMSO was allowed to stand at room temperature to determine whether ligand exchange would occur. ESI-MS and ^{1}H NMR spectroscopy showed only a 1:1 mixture of homoleptic cages. There was no evidence of the formation of any heteroleptic species. Neither heating to 50 °C, overnight, nor standing for six months produced observable changes to the ESI-MS. A mixture of preformed $[Pd_6(\mathbf{L2})_8]\cdot 12\,BF_4$ and $[Pd_6(\mathbf{L2\,a})_8]\cdot 12\,BF_4$ showed that, after overnight heating then standing for two months, limited ligand exchange does occur with the exchange of up to three ligands, per cage, according to ESI-MS.

This is contrasting behaviour to that reported by Dalcanale and co-workers on similar types of cavitand-based metallocage systems.[24] They mixed two distinct homoleptic Pt_4L_2 cages where the L ligands were pyridyl-derived calix[4]resorcinarene cavitands with different lower-rim groups, and observed formation of heteroleptic cages in solution on heating and standing. Zheng and Stang have likewise shown that combinations of homoleptic Pt-based supramolecular polygons undergo dynamic ligand exchange to form mixtures of heteroleptic polygons.[25] Conversely, Fujita and co-workers have remarked on the high kinetic inertness displayed by much larger $Pd_{12}L_{24}$ metallo-cages,[26] and slow ligand exchange in metallo-cages has likewise been reported by both Raymond[27] and Ward.[28] Ward has also investigated metal exchange in $[M_4L_6]^{4+}$ metallo-cages, where $M = Co^{II}$ or Cd^{II}. They observed that metal scrambling began soon after mixing, and a near binomial distribution of $[Co_{4-n}Cd_nL_2]^{4+}$ species was achieved after 150 days.[29] Our results initially seemed more in keeping with those of Fujita, and attributable to the larger size of our cage compared with Dalcanale's, and the presence of more M-cavitand bonds (24 compared with 8). Additional experiments, however, revealed that the solution behaviour of the Pd_6L_8 cages is more complicated, and that under some conditions, formation of the $[Pd_6(\mathbf{L1\,a})_8]^{12+}$ cage is more favourable than formation of the $[Pd_6(\mathbf{L1})_8]^{12+}$ counterpart.

The addition of eight equivalents of methylated ligand **L1 a** to the preformed $[Pd_6(\mathbf{L1})_8]^{12+}$ assembly saw immediate conversion to the methylated cage $[Pd_6(\mathbf{L1\,a})_8]^{12+}$. The resultant ^{1}H NMR spectrum is an overlay of the spectra of **L1** and $[Pd_6(\mathbf{L1\,a})_8]^{12+}$ (Figure S28 in the Supporting Information). ESI-MS shows a clear bias towards **L1 a**-containing cages with the observation of $[Pd_6(\mathbf{L1})_{8-n}(\mathbf{L1\,a})_n]^{12+}$ species, where $n = 4$ to 8. Interestingly, ligand–cage adducts are also observed, which may indicate that the ligand exchange proceeds through an associative mechanism. The converse reaction, where preformed methylated $[Pd_6(\mathbf{L1\,a})_8]^{12+}$ is treated with propylated **L1** in DMSO, also shows a bias towards the methylated $[Pd_6(\mathbf{L1\,a})_8]^{12+}$ cage by ESI-MS and no ligand exchange was observable by NMR spectroscopy (Figure S29 in the Supporting Information).

This difference in cage favourability in the presence of additional ligand according to ligand identity, along with DMAP-induced chemical disassembly, allows us to control the predominant speciation in solution, summarised in Scheme 3. A mixture of heteroleptic $[Pd_6(\mathbf{L1})_{8-n}(\mathbf{L1\,a})_n]\cdot 12\,BF_4$ cages is generated from the combination of six equivalents of $[Pd(MeCN)_4](BF_4)_2$ with four equivalents of each of **L1** and **L1 a**, as there is insufficient **L1 a** in solution to only form the favoured $[Pd_6(\mathbf{L1\,a})_8]^{12+}$ cage. Addition of a further 4 equivalents of each of **L1** and **L1 a** to the same solution results in rapid, more selective cage formation with the methylated $[Pd_6(\mathbf{L1\,a})_8]^{12+}$ and free propylated ligand **L1** observed as the major species in solution by NMR spectroscopy. The addition of a further six equivalents of $[Pd(MeCN)_4](BF_4)_2$ returns the system to a cage mixture, although one that is strongly biased towards the homoleptic over heteroleptic species according to NMR spectroscopy and ESI-MS (Figure 6 and Scheme 3, respectively). Disassembly of

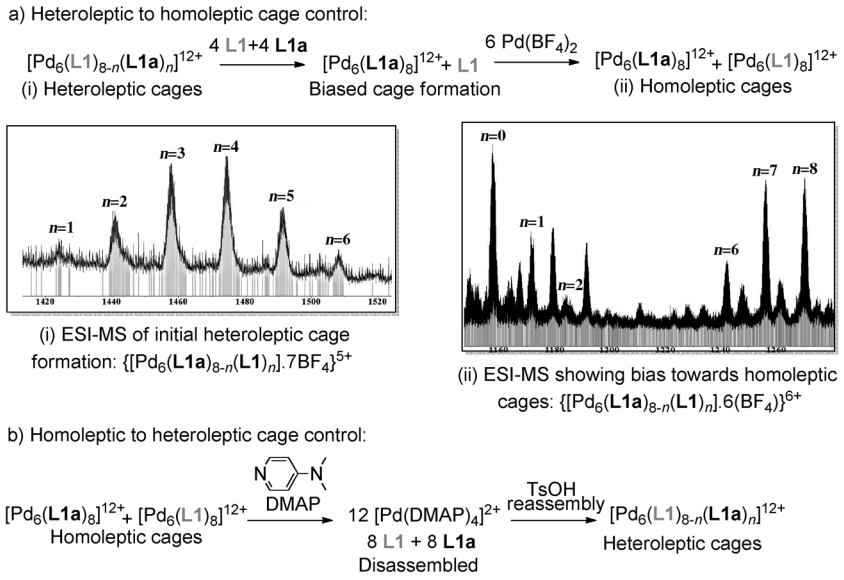

Scheme 3. Ligand speciation control of $[Pd_6L_8]^{12+}$ stella octangula cages through: a) stoichiometry; b) chemical disassembly and reassembly.

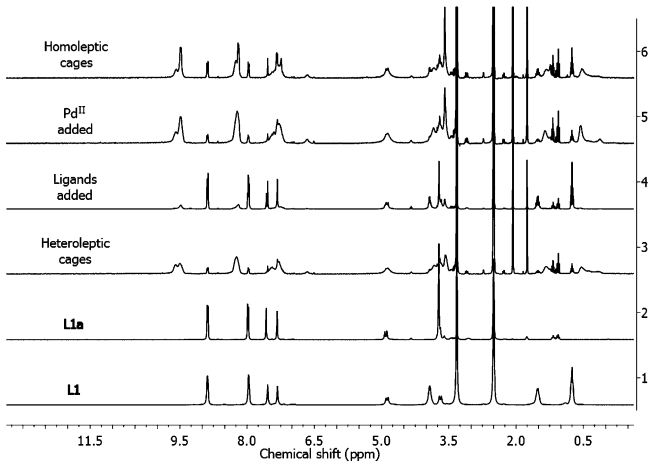

Figure 6. ^{1}H NMR of process of Scheme 3a. Speciation is changed from a mixture of heteroleptic cages to predominance of $[Pd_6(\mathbf{L1a})_8]^{12+}$ on addition of additional equivalents of both ligands, then to a mixture of homoleptic cages on addition of more $[Pd(MeCN)_4](BF_4)_2$ (marked "Pd^{II} added"). The top spectrum is a mixture of preformed homoleptic cages for comparison.

the 1:1 mixture of homoleptic cages can be affected using DMAP. Subsequent addition of TsOH reassembles the cages to once again form a mixture of heteroleptic cages, as the **L1**/**L1a**/Pd^{II} stoichiometric ratio in the disassembled solution is now 4:4:6 (Scheme 3). ESI-MS taken after this disassembly–reassembly process also gives evidence of ligand–cage adduct formation (Figure S34 in the Supporting Information).

Conclusion

The propylated ligands **L1** and **L2** form $[Pd_6L_8]^{12+}$ stella octangula metallo-cage species, and the first Pt^{II} stella octangula $[Pt_6(\mathbf{L1})_8]^{12+}$ was synthesised. As anticipated, the propyl $[Pd_6L_8]^{12+}$ cages have improved solubility over their previously reported methyl counterparts.[9] This is likely to be advantageous for host–guest studies and preliminary work showed that $[Pd_6(\mathbf{L1})_8]^{12+}$ associates with the spherical guest *o*-carborane.

The crystal structure of $[Pd_6(\mathbf{L1})_8]\cdot 12(BF_4)\cdot 2H_2O$ grown from DMSO solution was very disordered, with superposition of both enantiomers of the **L1** ligand, indicating no chiral self-sorting of the ligands. The broad ^{1}H NMR spectra for $[Pd_6(\mathbf{L1})_{12}]^{12+}$ in DMSO are also indicative of a mixture of cage isomers. This was not the case for $[Pd_6(\mathbf{L1})_{12}]^{12+}$ in MeCN or $MeNO_2$ in which sharpened spectra indicate self-sorting.

Despite the lability of Pd–N bonds, homoleptic mixtures of preformed $[Pd_6L_8]^{12+}$ stella octangula cages show no, or only very minor, ligand exchange in DMSO even after many months in solution. This is in keeping with studies on other large cage systems, where ligand exchange was observed to be slow,[26–28] although it is unusual to observe no exchange at all, as was the case for the $[Pd_6(\mathbf{L1})_8]^{12+}$ and $[Pd_6(\mathbf{L1a})_8]^{12+}$ mixture. The cages can be disrupted by addition of more ligand, and a significant degree of ligand exchange was seen on addition of **L1a** to $[Pd_6(\mathbf{L1})_8]^{12+}$. However, the degree of ligand exchange was considerably smaller when **L1** was added to $[Pd_6(\mathbf{L1a})_8]^{12+}$. This suggests that the $[Pd_6(\mathbf{L1a})_8]^{12+}$ cage is the favoured product over $[Pd_6(\mathbf{L1})_8]^{12+}$ on addition of excess ligand. The observation of ligand–cage adducts during ligand exchange experiments supports the notion that ligand exchange occurs through an associative mechanism. The favouring of $[Pd_6(\mathbf{L1a})_8]^{12+}$ in the presence of additional ligand may therefore reflect that **L1a** has less sterically demanding methyl groups on its upper rim compared with the more sterically demanding propyl groups of **L1**.

The formation of near binomial mixtures of heteroleptic cages from 4:4:6 **L1**/**L1a**/Pd^{II} mixtures (and from **L2**/**L2a** counterpart) is as expected from the solution stoichiometry and indicates kinetic control. Addition of more ligand biases the system to $[Pd_6(\mathbf{L1a})_8]^{12+}$, which is consistent with ligand exchange experiments described above. This leaves more **L1** in solution than **L1a**, which favours a homoleptic cage distribution on addition of more equivalents of Pd^{II}. This allows us to exercise a degree of control over the predominant species in solution.

Experimental Section

Synthesis

(±)-2,7,12-Tripropoxy-3,8,13-trimethoxy-10,15-dihydro-5*H*-tribenzo-[*a,d,g*]cyclononene (**1**),[14] lithium diphenylphosphide,[13] 4-(4-pyridyl)benzoyl chloride hydrochloride[9a] *tris*(isonicotinoyl)cyclotriguaiacylene (**1a**)[16] and *tris*(4-pyridyl-4-benzoxy)cyclotriguaiacylene (**2a**)[9b] were prepared according to literature methods. Reagents were obtained from commercial sources and were used as received.

(±)-2,7,12-Tripropoxy-3,8,13-trihydroxy-10,15-dihydro-5*H*-tribenzo[*a,d,g*]cyclononene (2): (±)-2,7,12-Tripropoxy-3,8,13-trimethoxy-10,15-dihydro-5*H*-tribenzo[*a,d,g*]cyclononene (**1**; 2.01 g, 3.74 mmol) and anhydrous THF (10 mL) were added to a flame-dried Schlenk tube and stirred vigorously. Lithium diphenylphosphide was added dropwise via cannulae transfer over 2 h, during which time it decolourised. The reaction mixture was stirred, overnight, and solidified. The resultant lithium phenoxide was hydrolysed with concentrated aq. HCl and volatiles were removed in vacuo. Organics were extracted into dichloromethane (6×100 mL) and then back-extracted with 6 M aqueous sodium hydroxide (6×100 mL). The sodium hydroxide layer was washed with dichloromethane (4×100 mL) and acidified with 6 M aqueous HCl to precipitate the desired product as an off-white solid. The solid was allowed to stand for 1 h before being filtered, washed with water (2×50 mL) and dried. Subsequent dissolution of the solid in chloroform, filtration through a silica pad and evaporation of the solution afforded the title compound as a colourless glass. Yield 974 mg, 55%. M.p. decomposes >270 °C; ^{1}H NMR (300 MHz, $CDCl_3$, 25 °C, TMS): δ = 8.52 (s, 3H; phenol), 6.82 (s, 3H; aryl-H), 6.80 (s, 3H; aryl-H), 4.55 (d, J = 13.4 Hz, 3H; CTG *exo*-H), 3.86 (t, J = 6.6 Hz, 6H; propyl Σ-H), 3.31 (d, J = 13.4 Hz, 3H; CTG *endo*-H), 1.69 (q, J = 7.2 Hz, 6H; propyl β-H), 0.96 ppm (t, J = 7.4 Hz, 9H; propyl Y-H); ^{13}C{^{1}H} NMR (75 MHz, $CDCl_3$, 25 °C, TMS): δ = 145.2, 145.0, 132.6, 130.4, 116.7, 115.3, 70.2, 35.0, 22.1, 10.4 ppm; IR (FT-IR): $\tilde{\nu}$ = 3550–3110 (broad), 2945, 2910, 1645, 1485, 1390 cm^{-1}; HRMS (ESI+): *m/z* calcd for $[M+Na]^+$: 515.2410; found: 515.2410; elemental analysis calcd (%) for $C_{30}H_{36}O_6 \cdot 0.5(H_2O)$: C 71.83, H 7.43; found: C 72.15, H 7.35.

(±)-2,7,12-Tripropoxy-3,8,13-*tris*(4-pyridylcarboxy)-10,15-dihydro-5*H*-tribenzo[*a,d,g*]cyclononene (*tris*(isonicotinoyl)-*tris*-(propyl)-cyclotricatechylene) (L1): Anhydrous triethylamine (2.4 mL, 13.56 mmol) was added to a stirred solution of 2 (555 mg, 1.13 mmol) in anhydrous THF (150 mL), at −78 °C, under an argon atmosphere. After 1 h, isonicotinoyl chloride hydrochloride (800 mg, 4.50 mmol) was added to the reaction mixture and stirred at −78 °C for a further 2 h before being left at RT for 48 h. A second portion of isonicotinoyl chloride hydrochloride (800 mg, 4.50 mmol) was added, and left to stir for a further 48 h, during which time the reaction mixture discoloured. The solvent was removed in vacuo and the resultant residue triturated in ethanol to afford the target compound as a white solid, which was isolated by filtration and dried in vacuo. Yield 640 mg, 66%. M.p. decomposes >270 °C; ^{1}H NMR (500 MHz, $CDCl_3$, 25 °C, TMS): δ = 8.84 (d, J = 6.0 Hz, 6H; Py-H^2), 7.97 (d, J = 6.0 Hz, 6H; Py-H^3), 7.16 (s, 3H; aryl-H), 6.94 (s, 3H; aryl-H), 4.82 (d, J = 13.6 Hz, 3H; CTG *exo*-H), 3.93 (t, J = 6.2 Hz, 6H; propyl Σ-H), 3.67 (d, J = 13.6 Hz, 3H; CTG *endo*-H), 1.66 (q, J = 7.4 Hz, 6H; propyl β-H), 0.86 ppm (t, J = 7.2 Hz, 9H; propyl Y-H); ^{13}C{^{1}H} NMR (75 MHz, $CDCl_3$, 25 °C, TMS): δ = 162.6, 149.6, 148.2, 138.9, 137.9, 137.5, 131.9, 123.8, 123.6, 115.5, 69.8, 34.9, 21.7, 10.1 ppm; IR (FT-IR): $\tilde{\nu}$ = 3100, 2875, 1745 (strong), 1605, 1520 cm^{-1}; HRMS (ESI+): *m/z* calcd for $[M+H]^+$: 808.3234; found: 808.3232; elemental analysis calcd (%) for $C_{30}H_{36}O_6 \cdot (H_2O)$: C 69.80, H 5.74, N 5.09; found: C 70.00, H 5.55, N 4.80.

(±)-2,7,12-Tripropoxy-3,8,13-*tris*(4-pyridyl-4-phenylcarboxy)-10,15-dihydro-5*H*-tribenzo[*a,d,g*]cyclononene (*tris*(4-pyridyl-4-benzoxy)-*tris*(propyl)-cyclotricatechylene) (L2): Anhydrous triethylamine (1.32 mL, 7.56 mmol) was added to a stirred solution of **2** (310 mg, 0.630 mmol) in anhydrous THF (50 mL), at −78 °C, under an argon atmosphere. After 1 h, 4-(4-pyridyl)benzoylchloride hydrochloride (960 mg, 3.78 mmol) was added to the reaction mixture and stirred at −78 °C for a further 2 h before being left at RT for 48 h. The solvent was removed in vacuo and the resultant residue was triturated in ethanol to afford the target compound as a white solid, which was isolated by filtration and dried in vacuo. Yield 609 mg, 93%. M.p. decomposes >270 °C; ^{1}H NMR (300 MHz, [D$_6$]DMSO, 25 °C): δ = 8.70 (d, J = 6.2 Hz, 6H; Py-H^2), 8.20 (d, J = 8.5 Hz, 6H, Ph-H^3), 8.03 (d, J = 8.5 Hz, 6H; Ph-H^2), 7.81 (d, J = 6.2 Hz, 6H; Py-H^3), 7.53 (s, 3H; aryl-H), 7.34 (s, 3H; aryl-H), 4.87 (d, J = 12.5 Hz, 3H; CTG *exo*-H), 3.94 (t, J = 6.2 Hz, 6H; propyl Σ-H), 3.73 (d, J = 12.5 Hz, 3H; CTG *endo*-H), 1.53 (q, J = 6.6 Hz, 6H; propyl β-H), 0.78 ppm (t, J = 7.4 Hz, 9H; propyl Y-H); ^{13}C{^{1}H} NMR (75 MHz, [D$_6$]DMSO, 25 °C): δ = 184.2, 150.7, 148.6, 145.7, 142.2, 138.4, 136.6, 131.8, 130.3, 129.2, 127.2, 121.5, 69.7, 21.8, 9.9 ppm; IR (FT-IR): $\tilde{\nu}$ = 2960, 1734 (s), 1594, 1508, 1400, 1263 (s), 1181, 1093, 820, 762 cm^{-1}; HRMS (ESI+): *m/z* calcd for $[M+Na]^+$: 1058.3993; found: 1058.3941; elemental analysis calcd (%) for $C_{66}H_{57}N_3O_9 \cdot 0.5(CHCl_3)$: C 72.88, H 5.29, N 3.83; found: C 73.15, H 5.40, N 3.80.

$[Pd_6(L1)_8]\cdot 12(BF_4)\cdot n$(MeCN) stella octangula: $[Pd(MeCN)_4](BF_4)_2$ (5.0 mg, 0.0113 mmol) and **L1** (12.10 mg, 0.0150 mmol) were dissolved in [D$_3$]MeCN (~2 mL) and stirred for 1 h, resulting in a pale-yellow solution, whereby ^{1}H NMR spectroscopy displayed quantitative cage formation. Diffusion of diethyl ether vapour into the solution afforded small, yellow prisms that were isolated, washed with a portion of diethyl ether and dried in vacuo. Quantitative ^{1}H NMR (300 MHz, [D$_3$]MeCN, 25 °C): δ = 9.31 (m, 1H; Py-H^2, achiral cage), 9.16 (d, 5H; Py-H^2, chiral cage), 8.13 (d, 6H; Py-H^3), 7.27 (s, 3H; aryl-H), 7.10 (s, 3H; aryl-H), 4.84 (d, 3H; CTG *exo*-H), 3.87 (m, 6H; propyl Σ-H), 3.69 (d, 3H; CTG *endo*-H), 1.62 (m, 1H; propyl β-H), 1.40 (m, 5H; propyl β-H), 0.85 (m, 2H; propyl Y-H), 0.60 ppm (m, 7H; propyl Y-H); IR (FT-IR): $\tilde{\nu}$ = 3494, 2968, 2901, 1751, 1619, 1508, 1270 cm^{-1} (s); HRMS (ESI+): *m/z* 1076.7391 $\{[Pd_6L_8]\cdot 5BF_4\}^{7+}$, 1270.3947 $\{[Pd_6L_8]\cdot 6BF_4\}^{6+}$, 1542.0858$\{[Pd_6L_8]\cdot 7BF_4\}^{5+}$ and 1949.6343 $\{[Pd_6L_8]\cdot 8BF_4\}^{4+}$; satisfactory elemental analysis could not be obtained owing to high levels of solvation.

$[Pt_6(L1)_8]\cdot 12(ClO_4)$ stella octangula: $Pt(ClO_4)_2$ (3.66 mg, 0.00928 mmol) was added to a solution of **L1** (10.12 mg, 0.0124 mmol) in [D$_6$]DMSO (1 mL) and stirred at 70 °C, overnight. ^{1}H NMR spectroscopy on the cooled solution displayed partial cage formation (~75% based on relative integrals). ^{1}H NMR (300 MHz, [D$_6$]DMSO, 25 °C): δ = 9.53–9.44 (bm, 3H; Py-H^2), 9.16 (d, 3H; Py-H^2), 8.88 (d; free **L1**), 8.33–8.25 (bm, 6H; Py-H^3), 7.96 (d; free **L1**), 7.55 (s, 3H; aryl-H), 7.32 (s, 3H; aryl-H), 4.89 (bd, 3H; CTG *exo*-H), 3.93 (bm, 6H; propyl Σ-H), 3.70 (bd, 3H; CTG *endo*-H), 1.53 (q; free **L1**), 1.30 (bq, 6H; propyl β-H), 0.75 (t; free **L1**), 0.53 ppm (m, 9H; propyl Y-H); HRMS (ESI+): *m/z* 1371.6856 $\{[Pt_6L_8]\cdot 6ClO_4\}^{6+}$, 1665.9895 $\{[Pt_6L_8]\cdot 7ClO_4\}^{5+}$ and 2107.4224 $\{[Pt_6L_8]\cdot 8ClO_4\}^{4+}$.

$[Pd_6(L2)_8]\cdot 12(BF_4)$ stella octangula: $[Pd(MeCN)_4](BF_4)_2$(3.2 mg, 0.00725 mmol) and **L2** (10.00 mg, 0.00966 mmol) were dissolved in [D$_6$]DMSO (~2 mL) and stirred for 1 h, resulting in a pale-yellow solution, where both 1D and 2D ^{1}H NMR spectroscopy displayed cage formation. Diffusion of acetone vapour into the solution afforded a microcrystalline solid which was isolated, washed with a portion of acetone and dried in vacuo. ^{1}H NMR (300 MHz, [D$_6$]DMSO, 25 °C): δ = 9.34 (bm, 6H; Py-H^2), 8.24–8.08 (bm, 18H; Py-

H^3, Ph-H^2, Ph-H^3), 7.46 (s, 3H; aryl-H), 7.30 (s, 3H; aryl-H), 4.82 (bd, 3H; CTG *exo*-H), 3.84 (bm, 6H; propyl Σ-H), 3.69 (bd, 3H; CTG *endo*-H), 1.38 (bq, 6H; propyl β-H), 0.61 ppm (bt, 9H; propyl Y-H); IR (FT-IR): $\tilde{\nu}=3384$ (broad), 1742 (weak), 1622 (weak), 1024 cm^{-1} (weak); HRMS (ESI+): *m/z* 1020.9683 $\{[Pd_6L_8]\cdot 3BF_4\}^{9+}$, 1159.3551 $\{[Pd_6L_8]\cdot 4BF_4\}^{8+}$, 1337.3494 $\{[Pd_6L_8]\cdot 5BF_4\}^{7+}$, 1574.9554 $\{[Pd_6L_8]\cdot 6BF_4\}^{6+}$ and 1906.9543 $\{[Pd_6L_8]\cdot 7BF_4\}^{5+}$; satisfactory elemental analysis could not be obtained due to high levels of solvation.

X-ray crystallography

Crystals were mounted on MiTeGen loops under oil and flash frozen under N_2. Data were collected on a Bruker X8 diffractometer with $Mo_{K\alpha}$ radiation ($\lambda=0.71073$ Å) or on a Rigaku Saturn diffractometer with synchrotron radiation ($\lambda=0.6889$ Å) at station I19 of the Diamond Light Source. Data were corrected for absorption using a multiscan method, and structures were solved by direct methods and refined by full-matrix least squares on F^2 using the SHELX suite of programs,[30] interfaced through the program X-Seed.[31] Summaries of refinements are given below, full details are available in the Supporting Information.

L1·0.5 ($MeNO_2$)·1.5 (H_2O): $C_{48.5}H_{50.5}N_{3.5}O_{11.5}$: $M_r=866.42$, triclinic, space group $P\bar{1}$, $a=13.506(2)$, $b=15.49593)$, $c=16.120(3)$ Å, $\alpha=62.596(8)$, $\beta=65.374(8)$, $\gamma=64.841(8)^\circ$; $V=2606.2(8)$ Å^3; $Z=2$; $\theta_{max}=22.98^\circ$; data/restraints/parameters: 6798/4/572; R_1(obs. data) = 0.1777.

[Pd_6(L1)$_8$]·12 (BF_4)·6 (H_2O): $C_{228}H_{228}B_{12}F_{48}N_{24}O_{54}Pd_6$: $M_r=6629.54$, tetragonal, space group *I*4/*mmm*, $a=30.688(5)$, $c=45.906(11)$ Å; $V=43234(15)$ Å^3; $Z=2$; $\theta_{max}=20.00^\circ$; data/restraints/parameters: 6101/0/90; R_1(obs. data) = 0.1577. Structure showed significant disorder and most aromatic rings were refined with a rigid body constraint, propyl groups and anions were not located in the difference map (in the Supporting Information). There were large solvent-accessible voids hence the data were treated with the SQUEEZE routine of PLATON.[32]

CCDC-955885 (**L1**·0.5 ($MeNO_2$)·1.5 (H_2O)) and -971406 ([Pd_6(**L1**)$_8$]·12 (BF_4)·6 (H_2O)) contain the supplementary crystallographic data for this paper. These data can be obtained free of charge from The Cambridge Crystallographic Data Centre via www.ccdc.cam.ac.uk/data_request/cif.

Acknowledgements

We thank the EPSRC and the Brotherton Trust (JJH) for funding, I. Blakeley for microanalysis and N. Cookson for helpful discussions. This work was carried out with the support of the Diamond Light Source for time in station I19 under proposal mt7847.

Keywords: coordination cage · ligand exchange · self-assembly · self-sorting · supramolecular chemistry

[1] For reviews, see: a) S. R. Seidel, P. J. Stang, *Acc. Chem. Res.* **2002**, *35*, 972–983; b) M. Fujita, K. Umemoto, M. Yoshizawa, N. Fujita, T. Kusukawa, K. Biradha, *Chem. Commun.* **2001**, 509–518; c) D. L. Caulder, K. N. Raymond, *Acc. Chem. Res.* **1999**, *32*, 975–982.

[2] For example: a) P. Mal, B. Breiner, K. Rissanen, J. R. Nitschke, *Science* **2009**, *324*, 1697; b) M. Yoshizawa, T. Kusukawa, M. Fujita, K. Yamaguchi, *J. Am. Chem. Soc.* **2000**, *122*, 6311.

[3] For example: a) Z. J. Wang, K. N. Clary, R. G. Bergman, K. N. Raymond, F. D. Toste, *Nat. Chem.* **2013**, *5*, 100–103; b) C. J. Brown, G. M. Miller, M. W. Johnson, R. G. Bergman, K. N. Raymond, *J. Am. Chem. Soc.* **2011**, *133*, 11964–119466; c) M. Yoshizawa, J. K. Klosterman, M. Fujita, *Angew. Chem.* **2009**, *121*, 3470–3490; *Angew. Chem. Int. Ed.* **2009**, *48*, 3418–3438; d) Z. Yan, T. McCracken, S. Xia, V. Maslak, J. Galluci, C. M. Hadad, J. D. Badjic, *J. Org. Chem.* **2008**, *73*, 355–363; e) M. Yoshizawa, M. Tamura, M. Fujita, *Science* **2006**, *312*, 251–254.

[4] T. Ichijo, S. Sato, M. Fujita, *J. Am. Chem. Soc.* **2013**, *135*, 6786–6789.

[5] For examples and reviews, see: a) S. Pasquale, S. Sattin, E. C. Escudero-Adán, M. Martínez-Belmonte, J. de Mendoza, *Nat. Commun.* **2012**, *3*, 785; b) T. Schröder, S. N. Sahu, J. Mattay, *Top. Curr. Chem.* **2012**, *319*, 99–124; c) R. Pinalli, F. Boccini, E. Dalcanale, *Isr. J. Chem.* **2011**, *51*, 781–797; d) P. Jin, S. J. Dalgarno, J. L. Atwood, *Coord. Chem. Rev.* **2010**, *254*, 1760–1768; e) T. Haino, M. Kobayashi, Y. Fukuzawa, *Chem. Eur. J.* **2006**, *12*, 3310–3319; f) H. Jude, D. J. Sinclair, N. Das, M. S. Sherburn, P. J. Stang, *J. Org. Chem.* **2006**, *71*, 4155–4163; g) O. D. Fox, J. Cookson, E. J. S. Wilkinson, M. G. B. Drew, E. J. MacLean, S. J. Teat, P. D. Beer, *J. Am. Chem. Soc.* **2006**, *128*, 6990–7002; h) R. M. McKinlay, G. W. V. Cave, J. L. Atwood, *Proc. Natl. Acad. Sci. USA* **2005**, *102*, 5944–5948; i) E. Menozzi, M. Busi, R. Ramingo, M. Campagnolo, S. Geremia, E. Dalcanale, *Chem. Eur. J.* **2005**, *11*, 3136–3148; j) K. Kobayashi, Y. Yamada, M. Yamanaka, Y. Sei, K. Yamaguchi, *J. Am. Chem. Soc.* **2004**, *126*, 13896–13897; k) L. Baldini, P. Ballester, A. Casnati, R. M. Gomila, C. A. Hunter, F. Sansone, R. Ungaro, *J. Am. Chem. Soc.* **2003**, *125*, 14181–14189; l) O. D. Fox, N. K. Dalley, R. G. Harrison, *J. Am. Chem. Soc.* **1998**, *120*, 7111–7112.

[6] For review, see: M. J. Hardie, in *Supramolecular Chemistry: from Molecules to Nanomaterials, Vol. 3* (Eds.: P. A. Gale, J. W. Steed), **2012**, Wiley, pp. 895–916.

[7] a) J. J. Henkelis, T. K. Ronson, L. P. Harding, M. J. Hardie, *Chem. Commun.* **2011**, *47*, 6560–6562; b) T. K. Ronson, H. Nowell, A. Westcott, M. J. Hardie, *Chem. Commun.* **2011**, *47*, 176–178; c) A. Westcott, J. Fisher, L. P. Harding, P. Rizkallah, M. J. Hardie, *J. Am. Chem. Soc.* **2008**, *130*, 2950–2951; d) Z. Zhong, A. Ikeda, S. Shinkai, S. Sakamoto, K. Yamaguchi, *Org. Lett.* **2001**, *3*, 1085–1087.

[8] a) B. F. Abrahams, N. J. FitzGerald, R. Robson, *Angew. Chem.* **2010**, *122*, 2958–2961; *Angew. Chem. Int. Ed.* **2010**, *49*, 2896–2899; b) C. J. Sumby, M. J. Carr, A. Franken, J. D. Kennedy, C. A. Kilner, M. J. Hardie, *New J. Chem.* **2006**, *30*, 1390–1396; c) C. J. Sumby, J. Fisher, T. J. Prior, M. J. Hardie, *Chem. Eur. J.* **2006**, *12*, 2945–2959.

[9] a) T. K. Ronson, C. Carruthers, J. Fisher, T. Brotin, L. P. Harding, P. J. Rizkallah, M. J. Hardie, *Inorg. Chem.* **2010**, *49*, 675–685; b) T. K. Ronson, J. Fisher, L. P. Harding, M. J. Hardie, *Angew. Chem.* **2007**, *119*, 9244–9246; *Angew. Chem. Int. Ed.* **2007**, *46*, 9086–9088.

[10] T. K. Ronson, J. Fisher, L. P. Harding, P. J. Rizkallah, J. E. Warren, M. J. Hardie, *Nat. Chem.* **2009**, *1*, 212–216.

[11] X. Xu, R. Warmuth, *J. Am. Chem. Soc.* **2008**, *130*, 7520–7521.

[12] For example a) A. Kraszewska, P. Rivera-Fuentes, G. Rapenne, J. Crassous, A. G. Petrovic, J. L. Alonso-Gomez, E. Huerta, F. Diederich, C. Thilgen, *Eur. J. Org. Chem.* **2010**, 4402–4411; b) T. Brotin, V. Roy, J.-P. Dutasta, *J. Org. Chem.* **2005**, *70*, 6187–6195; c) A. Arduini, F. Calzavacca, D. Demuru, A. Pochini, A. Secchi, *J. Org. Chem.* **2004**, *69*, 1386–1388; d) R. M. Thomas, D. S. Iyengar, *Synth. Commun.* **1999**, *29*, 2507–2509.

[13] a) J. Canceill, L. Lacombe, A. Collet, *J. Chem. Soc. Chem. Commun.* **1987**, 219–221; b) J. Canceill, A. Collet, J. Gabard, G. Gottarelli, G. P. Spada, *J. Am. Chem. Soc.* **1985**, *107*, 1299–1308.

[14] R. Ahmad, M. J. Hardie, *Supramol. Chem.* **2006**, *18*, 29–38.

[15] a) A. Westcott, C. J. Sumby, R. D. Walshaw, M. J. Hardie, *New J. Chem.* **2009**, *33*, 902–912; b) D. Bardelang, F. Camerel, R. Ziessel, M. Schmutz, M. J. Hannon, *J. Mater. Chem.* **2008**, *18*, 489–494; c) Y. Kubo, W. Yoshizumi, T. Minami, *Chem. Lett.* **2008**, *37*, 1238–1239.

[16] M. J. Hardie, C. J. Sumby, *Inorg. Chem.* **2004**, *43*, 6872–6874.

[17] Unit cell of [Pd_6(**L1 a**)$_8$]·12 (NO_3) tetragonal, space group *P*4/*n*, $a=32.5130(6)$, $c=31.5740(13)$ Å.[9b]

[18] M. Yoneya, T. Yamaguchi, S. Sato, M. Fujita, *J. Am. Chem. Soc.* **2012**, *134*, 14401–14407.

[19] For example: a) C. Gütz, R. Hovorka, G. Schnakenburg, A. Lützen, *Chem. Eur. J.* **2013**, *19*, 10890–10894; b) M. M. Safont-Sempere, G. Fernández, F. Würthner, *Chem. Rev.* **2011**, *111*, 5784–5814; c) C. G. Claessens, I. Sánchez-Molina, T. Torres, *Supramol. Chem.* **2009**, *21*, 44–47; d) U. Kiehne, T. Weilandt, A. Lützen, *Eur. J. Org. Chem.* **2008**, 2056–2064; e) I.-W. Hwang, T. Kamada, D. M. Ko, T. Nakamura, A. Tsuda, A. Osuka, D. Kim, *J. Am. Chem. Soc.* **2004**, *126*, 16187–16198; f) A. Lützen,

M. Hapke, J. Griep-Raming, D. Haase, W. Saak, *Angew. Chem.* **2002**, *114*, 2190 – 2194; *Angew. Chem. Int. Ed.* **2002**, *41*, 2086 – 2089; g) J.-M. Vincent, C. Philouze, I. Pianet, J.-B. Verlhac, *Chem. Eur. J.* **2000**, *6*, 3595 – 3599; h) M. A. Masood, E. J. Enemark, T. D. P. Stack, *Angew. Chem.* **1998**, *110*, 973 – 977; *Angew. Chem. Int. Ed.* **1998**, *37*, 928 – 932.

[20] A. Martinez, V. Robert, H. Gornitzka, J.-P. Dutasta, *Chem. Eur. J.* **2010**, *16*, 520 – 527.

[21] G. Cainelli, P. Galletti, D. Giacomini, *Chem. Soc. Rev.* **2009**, *38*, 990 – 1001.

[22] R. J. Blanch, M. Williams, G. D. Fallon, M. G. Gardiner, R. Kaddour, C. L. Raston, *Angew. Chem.* **1997**, *109*, 520 – 522; *Angew. Chem. Int. Ed. Engl.* **1997**, *36*, 504 – 506.

[23] a) J. E. M. Lewis, E. L. Gavey, S. A. Cameron, J. D. Crowley, *Chem. Sci.* **2012**, *3*, 778 – 784; b) J. D. Crowley, D. A. Leigh, P. J. Lusby, R. T. McBurney, L.-E. Perret-Aebi, C. Petzold, A. M. Z. Slawin, M. D. Symes, *J. Am. Chem. Soc.* **2007**, *129*, 15085 – 15090.

[24] L. Pirondini, F. Bertolini, B. Cantadori, F. Ugozzoli, C. Massera, E. Dalcanale, *Proc. Natl. Acad. Sci. USA* **2002**, *99*, 4911 – 4915.

[25] Y.-R. Zheng, P. J. Stang, *J. Am. Chem. Soc.* **2009**, *131*, 3487 – 3489.

[26] S. Sato, Y. Ishido, M. Fujita, *J. Am. Chem. Soc.* **2009**, *131*, 6064 – 6065.

[27] A. J. Terpin, M. Ziegler, D. W. Johnson, K. N. Raymond, *Angew. Chem.* **2001**, *113*, 161 – 164; *Angew. Chem. Int. Ed.* **2001**, *40*, 157 – 160.

[28] M. D. Ward, *Chem. Commun.* **2009**, 4487 – 4499.

[29] B. R. Hall, L. E. Manck, I. S. Tidmarsh, A. Stephenson, B. F. Taylor, E. J. Blaikie, D. A. van der Griend, M. D. Ward, *Dalton Trans.* **2011**, *40*, 12132 – 12145.

[30] G. M. Sheldrick, *Acta Crystallogr. Sect. A* **2008**, *64*, 112 – 122.

[31] L. J. Barbour, *Supramol. Chem.* **2001**, *1*, 189 – 191.

[32] A. L. Spek, *Acta Crystallogr. Sect. A* **1990**, *46*, C34.

Received: November 12, 2013
Published online on March 3, 2014